Draft version August 24, 2009
Preprint typeset using LaTeX style emulateapj v. 03/07/07

CANGAROO-III SEARCH FOR TEV GAMMA-RAYS FROM TWO CLUSTERS OF GALAXIES

R. Kiuchi[1], M. Mori[1], G. V. Bicknell[2], R. W. Clay[3], P. G. Edwards[4], R. Enomoto[1], S. Gunji[5], S. Hara[6], T. Hara[7], T. Hattori[8], S. Hayashi[9], Y. Higashi[10], Y. Hirai[11], K. Inoue[5], C. Itoh[6], S. Kabuki[10], F. Kajino[9], H. Katagiri[12], A. Kawachi[8], T. Kifune[1], H. Kubo[10], J. Kushida[8], Y. Matsubara[13], T. Mizukami[10], Y. Mizumoto[14], R. Mizuniwa[8], H. Muraishi[15], Y. Muraki[13], T. Naito[7], T. Nakamori[16], S. Nakano[10], D. Nishida[10], K. Nishijima[8], M. Ohishi[1], Y. Sakamoto[8], A. Seki[8], V. Stamatescu[3], T. Suzuki[11], D. L. Swaby[3], T. Tanimori[10], G. Thornton[3], F. Tokanai[5], K. Tsuchiya[17], S. Watanabe[10], Y. Yamada[9], E. Yamazaki[8], S. Yanagita[11], T. Yoshida[11], T. Yoshikoshi[1], and Y. Yukawa[1]

Draft version August 24, 2009

ABSTRACT

Because accretion and merger shocks in clusters of galaxies may accelerate particles to high energies, clusters are candidate sites for the origin of ultra-high-energy (UHE) cosmic-rays. A prediction was presented for gamma-ray emission from a cluster of galaxies at a detectable level with the current generation of imaging atmospheric Cherenkov telescopes. The gamma-ray emission was produced via inverse Compton upscattering of cosmic microwave background (CMB) photons by electron-positron pairs generated by collisions of UHE cosmic rays in the cluster. We observed two clusters of galaxies, Abell 3667 and Abell 4038, searching for very-high-energy gamma-ray emission with the CANGAROO-III atmospheric Cherenkov telescope system in 2006. The analysis showed no significant excess around these clusters, yielding upper limits on the gamma-ray emission. From a comparison of the upper limit for the north-west radio relic region of Abell 3667 with a model prediction, we derive a lower limit for the magnetic field of the region of $\sim 0.1 \mu$G. This shows the potential of gamma-ray observations in studies of the cluster environment. We also discuss the flux upper limit from cluster center regions using a model of gamma-ray emission from neutral pions produced in hadronic collisions of cosmic-ray protons with the intra-cluster medium (ICM). The derived upper limit of the cosmic-ray energy density within this framework is an order of magnitude higher than that of our Galaxy.

Subject headings: galaxies:clusters: individual(Abell 3667, Abell 4038) — gamma rays: observations — galaxies: magnetic fields

1. INTRODUCTION

Clusters of galaxies are the largest systems in the Universe that are gravitationally bound, and they are potential sources of ultra-high-energy (UHE) cosmic rays, since their sizes and moderate magnetic fields allow a high maximum energy ($\sim 10^{20}$ eV) in acceleration (Ostrowski 2002). Although cluster accretion and merger shocks could produce such high-energy particles, accretion shocks may be more effective than merger shocks in particle acceleration, due to their high Mach numbers (Miniati et al. 2000; Ryu et al. 2003). Cosmic-ray electrons accelerated directly by these shocks may produce gamma-ray emission via inverse Compton (IC) scattering of the cosmic microwave background (CMB) (Totani & Kitayama 2000; Miniati 2003; Gabici & Blasi 2004). On the other hand, accelerated cosmic ray protons can interact hadronically with the intra-cluster medium (ICM), and gamma-rays may be produced via π^0-decay (Völk et al. 1996; Berezinsky et al. 1997; Pfrommer & Enßlin 2004) as well as IC emission by secondary electron/positron pairs from $\pi^{\pm}$-decay (Blasi & Colafrancesco 1999).

Observations of clusters of galaxies at various wavelengths (e.g., radio, EUV, X-ray) suggest the existence of non-thermal particles in these gigantic objects (Fusco-Femiano et al. 2001; Nevalainen et al. 2004; Bowyer et al. 2004; Giovannini & Feretti 2004). However, at gamma-ray energies, no observational evidence has been reported from clusters of galaxies (Reimer et al. 2003), though there is suggestive evidence (Kawasaki & Totani

[1] Institute for Cosmic Ray Research, University of Tokyo, Kashiwa, Chiba 277-8582, Japan
[2] Research School of Astronomy and Astrophysics, Australian National University, ACT 2611, Australia
[3] School of Chemistry and Physics, University of Adelaide, SA 5005, Australia
[4] CSIRO Australia Telescope National Facility, Narrabri, NSW 2390, Australia
[5] Department of Physics, Yamagata University, Yamagata, Yamagata 990-8560, Japan
[6] Ibaraki Prefectural University of Health Sciences, Ami, Ibaraki 300-0394, Japan
[7] Faculty of Management Information, Yamanashi Gakuin University, Kofu, Yamanashi 400-8575, Japan
[8] Department of Physics, Tokai University, Hiratsuka, Kanagawa 259-1292, Japan
[9] Department of Physics, Konan University, Kobe, Hyogo 658-8501, Japan
[10] Department of Physics, Kyoto University, Sakyo-ku, Kyoto 606-8502, Japan
[11] Faculty of Science, Ibaraki University, Mito, Ibaraki 310-8512, Japan
[12] Department of Physical Science, Hiroshima University, Higashi-Hiroshima, Hiroshima 739-8526, Japan
[13] Solar-Terrestrial Environment Laboratory, Nagoya University, Nagoya, Aichi 464-8602, Japan
[14] National Astronomical Observatory of Japan, Mitaka, Tokyo 181-8588, Japan
[15] School of Allied Health Sciences, Kitasato University, Sagamihara, Kanagawa 228-8555, Japan
[16] Department of Basic Physics, Tokyo Institute of Technology, Meguro, Tokyo 152-8551, Japan
[17] National Research Institute of Police Science, Kashiwa, Chiba 277-0882, Japan

2002; Scharf & Mukherjee 2002). Observations in the TeV energy band with Imaging Atmospheric Cherenkov Telescope (hereafter IACT) experiments have yielded the only upper limits to date (Hattori et al. 2003; Fegan et al. 2005; Perkins et al. 2006; Domainko et al. 2007).

Recently, Inoue et al. (2005) considered protons, accelerated up to 10^{18}–10^{19} eV by accretion shocks around a massive cluster, interacting with the CMB photons, with secondary electron-positron pairs produced in the p-γ process, boosting those photons into the TeV energy range by IC scattering. Although their prediction depends on many physical parameters, the predicted gamma-ray flux could be at a detectable level for current IACT experiments for massive, nearby clusters. Thus, observations of clusters of galaxies with IACTs probe high-energy processes and the environment in these large-scale systems, and if gamma-ray signals are detected, they may also provide clues to help solve the mystery of UHE cosmic-ray production. If there is no detected signal, we can place limits on the physical parameters of clusters, such as the strength of the magnetic field.

In this paper we report on a search for TeV gamma-ray emission from two clusters of galaxies, Abell 3667 and Abell 4038, with CANGAROO-III, an array of imaging atmospheric Cherenkov telescopes. We selected these targets according to their high masses and relative closeness from the southern Abell catalog (Abell et al. 1989).

Abell 3667, also known as SC 2009-57, is classified as type L in the Rood-Sastry system (Rood & Sastry 1971) due to the linear arrangement of the galaxies, including two of the brightest D galaxies. The cluster has a redshift of $z = 0.055$ (Sodré et al. 1992), and is centered at $[\alpha(2000) = 20^h12^m27^s.4, \delta(2000) = -56°49'36"]$, which is the location of the brightest D galaxy (Knopp et al. 1996). The cluster is one of the brightest X-ray sources in the southern sky (Edge et al. 1992), and is also known to show significant diffuse radio emission around its center (Röttgering et al. 1997).

Abell 4038, also known as Klemola 44, is a rich southern cluster with $z = 0.028$, and is classified as type cD in the Rood-Sastry system, where the cD galaxy is centered at $[\alpha(2000) = 23^h47^m45^s.1, \delta(2000) = -28°08'26"]$ (Slee et al. 2001). An X-ray image shows an extended morphology, and there is a radio relic near the cD galaxy (Slee and Roy 1998), though it is smaller than the point spread function of typical IACTs ($\sim$0.1°).

The search described in the following sections focused on the detection of point sources within the cluster fields as well as looking for gamma-ray signals from several regions by assuming gamma-ray emission models: The giant radio relics around Abell 3667 may indicate the sites of shocks, where particle acceleration occurs effectively, and thus gamma-ray emission could be expected from the relics by the scenario of the UHE proton origin (Inoue et al. 2005). Apart from the shock regions, the density of the ICM is highest at the cluster centers, so the gamma-ray flux via π^0-decay would be strongest there.

In §2, we introduce the CANGAROO-III telescope systems and observations of the clusters. The data-analysis procedures are explained in §3, and the main results together with a definition of the gamma-ray search regions are described in §4. Finally, a discussion of the gamma-ray emission from clusters of galaxies based on the CANGAROO-III results is presented. Throughout this paper, we assume a Hubble constant of H_0=70 km s^{-1} Mpc^{-1}.

2. INSTRUMENT AND OBSERVATIONS

Two clusters of galaxies, Abell 3667 and Abell 4038, were observed in the TeV energy band using the imaging atmospheric Cherenkov technique with the CANGAROO-III telescope system (Enomoto et al. 2006a), located near Woomera, South Australia (136.786 degree E, 31.099 degree S, 160m a.s.l.). The system consists of four telescopes, which are located at the corners of a diamond with 100 m sides (Enomoto et al. 2002). The first telescope, which we call T1, was not used in these observations, since its current performance is inferior to that of the other telescopes. The specifications of the second, third, and fourth telescopes, hereafter called T2, T3, and T4, are almost the same: they have segmented paraboloid reflector 10 m in diameter and 8 m in focal length. Each reflector is composed of 114 spherical mirror facets, and the total mirror area is 54 m^2 (Kawachi et al. 2001). At each focus there is an imaging camera, which is an array of 427 photomultipliers (PMTs). Each PMT covers a sky field of 0.17° in diameter, and the total field-of-view is about 4°, suitable for applying analysis using an imaging technique (Kabuki et al. 2003). The data acquisition system is triggered when at least two telescopes have signals coinciding for more than 10 nsec within a 650 nsec time window, thus eliminating muon events that mostly trigger a single telescope (Nishijima et al. 2005). Then, the amplitude and the arrival times of signals from PMTs are digitized by ADC/TDC modules, and recorded for off-line analysis (Kubo et al. 2001).

The observations were carried out for ON-source and OFF-source tracking runs. For OFF-source runs, the target position was shifted in right ascension so that the telescopes tracked the same trajectory across the sky as ON-source runs. Also, we adopted *wobble mode* observations for both ON-source and OFF-source runs, in which the pointing direction was shifted in declination by ±0.5° from the target direction every 20 minutes. One of the advantages of the *wobble mode* is to average the response of PMTs, since the target position rotates on the FOV. All observations were made on moonless nights from July to September, 2006. Details of the data sets are summarized in Table 1.

In addition to the observations, we also observed dark regions (with no bright stars or gamma-ray sources in the field-of-view) without imposing the telescope coincidence described above, and we extracted local muon-ring events from these data to monitor the total performance of the telescopes (Enomoto et al. 2006a). This calibration (denoted *muon run*) was done every month, and their statistics are also shown in Table 1.

3. DATA ANALYSIS

We followed the analysis procedure explained in detail in Enomoto et al. (2006a), which we briefly describe here.

First, raw data were calibrated, using daily calibration runs using LEDs (Kabuki et al. 2003). We then selected the shower events from the calibrated datasets. For each triggered event, camera pixels that recorded less

TABLE 1
Summary of the data set used in this analysis.

Cluster	Term	ON[a] [hour]	OFF[a] [hour]	$\langle z \rangle$[b] [deg]
Abell 3667	Jul-Aug (2006)	29.7	23.7	28.6
Abell 4038	Aug-Sep (2006)	23.6	17.7	13.1
muon run	Jul-Sep (2006)	22.4	–	10.8

[a]Dead-time corrected observation time used in our analysis.
[b]Mean zenith angle of ON-source runs.

than 5 p.e. were discarded so as to remove any night-sky-background photons, and shower events were extracted from the remaining pixels, imposing the conditions that there were at least 5 adjacent hit pixels, and that the pixels were triggered within ±30 nsec from the mean arrival time of all hit pixels. This procedure cleaned the shower images and separated random noise, such as multiple night-sky-background photons. The typical shower event rate was ∼7 Hz (average over 5 minutes), and we excluded the data from the analysis when the shower event rate was below 5 Hz so as to remove any data affected by clouds etc. The effective total observation times for the selected datasets, taking account of the dead time in data acquisition, are summarized in Table 1. After this image-cleaning procedure, we discarded events with any hits in the outermost layer of the imaging cameras since such shower images may be distorted (Enomoto et al. 2006b).

Next, image moments (*width* and *length*) of showers were calculated as defined by Hillas (1985), and the arrival direction of the shower was reconstructed event by event, by minimizing the sum of the squared *widths* of the images weighted by their total photo-electron numbers seen from the assumed direction, as described in Kabuki et al. (2007).

Finally, gamma-ray/hadron separation was carried out by applying the Fisher discriminant method (Fisher 1936; Enomoto et al. 2006a). In this method, the Fisher discriminant (hereafter *FD*) is defined as a linear combination of the image moments,

$$FD = \sum_{i=1}^{6} \alpha_i \cdot P_i, \tag{1}$$

where $\mathbf{P} = (W_2, W_3, W_4, L_2, L_3, L_4)$ is a set of energy-corrected *width* and *length* of shower images of three telescopes. The coefficients, α_i ($i = 1\sim6$), were determined so that the difference of the *FD* distribution of gamma-ray events and that of hadron events would be maximized. We used Monte-Carlo simulation data as gamma-ray events, and OFF-source run data as background hadron events for deriving the coefficients. We then extracted gamma-ray events from ON-source run data by fitting the ON-source *FD* distribution with that of the background (OFF-source) distribution plus the gamma-ray distribution. Our Monte-Carlo simulation code is based on GEANT3, the details are described in Enomoto et al. (2002), where some parameters such as the geometry of the telescopes are replaced with those of the current CANGAROO-III system. The degradation of the overall light collection efficiency (including reflectivities of the reflectors, quantum efficiencies of photomultipliers, etc.) and the spot size of each telescope were estimated from a muon ring analysis (Enomoto et al. 2006a) using *muon run* data, and they were included in our simulation. In the gamma-ray simulation, we assumed a power-law spectrum index of $\gamma = -2.1$, which is often assumed for clusters of galaxies (e.g., Völk & Atoyan (2000)).

4. RESULTS

4.1. *Two dimensional morphology and θ^2 distribution*

First, we calculated the two-dimensional (2D) significance map around the cluster centers. We divided these (ON source) regions into $0.2^\circ \times 0.2^\circ$ square bins, and calculated the gamma-ray–like excesses and their errors with the *FD* fitting method, described in the previous section. Each background (OFF source run) bin was taken so that its position on the field of view would correspond to that of the ON region's bin, but the area was extended to 3×3 neighboring bins, to improve the statistical accuracy. Fig. 1 shows the resulting 2D significance maps of gamma-ray like excesses. Since the gamma-ray acceptance falls off toward the outer part of the field-of-view, we limit the map to within 1 degree from the cluster centers. The significance distributions from all bins in 2D maps were well approximated by standard normal distributions for both regions. The best fit Gaussians have mean values of 0.02±0.10 (Abell 3667) and 0.17±0.11 (Abell 4038), with standard deviations of 1.08±0.08 (Abell 3667) and 1.02±0.08 (Abell 4038), and there are no significant gamma-ray signals.

Next, we show the θ^2 distribution, where θ is the space angle between the target position and the reconstructed arrival direction, from the cluster centers in Fig. 2. The background bin for calculating each θ^2 bin was taken from the OFF source region to correspond to the position in the field of view. Although there were deviations in the θ^2 distributions, they were not significant ($<3\sigma$), considering our point-spread function ($\theta^2 < 0.06$ degree^2).
In summary, there were no detectable point sources in the cluster fields.

4.2. *Gamma-ray emission profiles and upper limits*

We also adopted several gamma-ray emission profiles in the cluster fields, and searched for diffuse gamma-ray emission. First, we defined two circular regions (hereafter *NW/SE Relic* regions) that cover the prominent radio relics around Abell 3667, since they may represent a shock morphology. The center coordinates (R.A. & Dec. in J2000) and their radii were defined as follows: $(20^h10^m24^s, -56^\circ27'00'')$ and 0.30° for the *NW Relic* region, $(20^h14^m36^s, -57^\circ03'00'')$ and 0.24° for the *SE Relic* region.

We expect that gamma-ray emission via π^0-decay is concentrated at the cluster center regions. It is well known that many clusters have a diffuse X-ray morphology at their centers, which may trace thermal components bounded by the gravitational potential of clusters. We thus assume that the gamma-ray emission profile traces the X-ray morphology of clusters. We adopted the *ROSAT* PSPC data for the X-ray morphology. The peak positions of the X-ray brightness are almost coincident with the cD galaxies of the clusters, which were

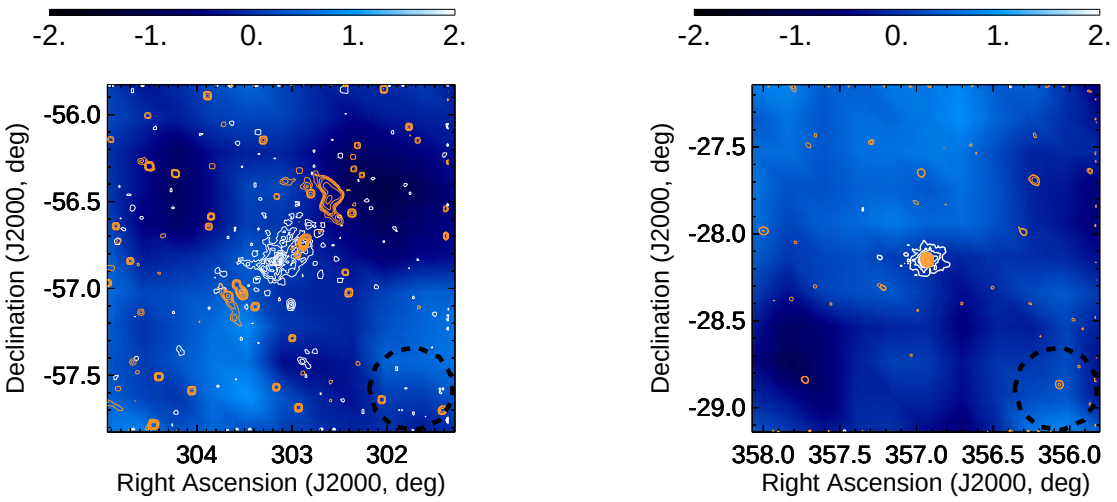

FIG. 1.— Two-dimensional significance maps around the clusters. The map centers correspond to the position of the cD galaxy of each cluster, and at each point a smoothing algorithm within $0.6^\circ \times 0.6^\circ$ was applied. Contours of other wavelengths (X-ray & radio) are over-plotted. The left panel is for Abell 3667, where the white contours show *ROSAT* hard-band data (Voges et al. 1999) and orange contours show SUMSS 843 MHz radio data (Mauch et al. 2003). The right panel is for Abell 4038, where white contours show *ROSAT* hard-band data and orange contours show VLA 1.4 GHz radio data (Condon et al. 1998). Our point-spread function is also shown at the bottom right-hand corner.

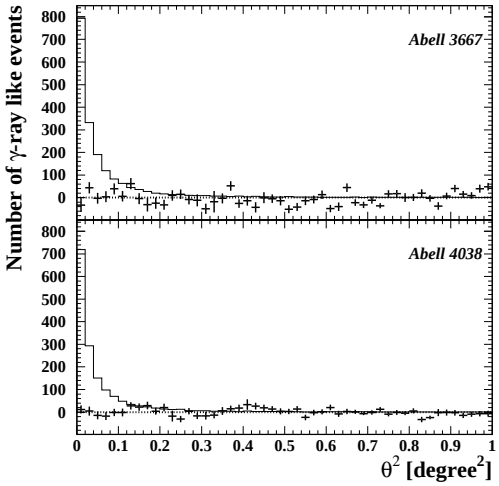

FIG. 2.— θ^2 distributions from cluster centers (where the definition of the center is the same as in Fig. 1). The upper panel is for Abell 3667 and the lower panel is for Abell 4038. The solid histograms show Monte-Carlo simulation results, assuming a Crab-nebula–level point-like gamma-ray source at each cluster center, and the dotted lines indicate the zero point. Note that our PSF corresponds to $\theta^2 < 0.06$ degree^2 .

the tracking points of our observations. We then defined two regions (hereafter *Cluster Core* regions), such that their centers were at the position of the cD galaxies and the radii were equal to the point where the S/N of the *ROSAT* data fell below ~ 3, which was 0.40° for Abell 3667 and 0.26° for Abell 4038, as described in Table 2 of Mohr et al. (1999). For Abell 3667, more recent observations with higher resolution have been reported (e.g., XMM-Newton (Briel et al. 2004); *Chandra* (Vikhlinin et al. 2001)). *Chandra* has a limited field-of-view for our purpose, however XMM showed that the signal region above the background noise level was in the central $11'$ which can be regarded as being a point source, considering the positional resolution of CANGAROO-III. So we first searched for gamma-ray signals from the Abell 3667 center region based on *ROSAT* data, and we later discuss the case of a point source, especially concerning the cosmic ray energy density. With the π^0-decay model, Völk & Atoyan (2000) assumed that the high-energy protons were accumulated in a cluster through supernova explosions, and that the predicted proton spectrum forms the power-law index $\Gamma = -2.1$ with an energy cutoff of E_{max}=200 TeV. So in our Monte-Carlo simulation, gamma-rays were generated uniformly within the defined area with a power-law spectrum having an index of $\gamma = -2.1$.

The gamma-ray events from each region were calculated by the *FD* fitting method, as before. The *FD* distribution of each region fitted with that of OFF-source region and that of gamma-ray events from a Monte-Carlo simulation is shown in Fig. 3. A gamma-ray signal would appear around *FD*=0 (see, e.g., Fig.1 in Enomoto et al. (2006b)); however, the calculated significances from the 4 regions did not exceed 3σ, and so there is no evidence of extended emission.

Therefore, we calculated the 2σ upper limits on the integral gamma-ray fluxes from these regions. The obtained flux upper limits, their threshold energy, and the definition of each region are summarized in Table 2.

5. DISCUSSION

Inoue et al. (2005) predicted gamma-ray emission at accretion shocks around a massive cluster. We searched for gamma-ray emission from radio relics of Abell 3667, assuming that they might trace the accretion shock (Enßlin et al. 1998), although it has also been suggested that the relics are the results of a major merger (Roettiger et al. 1999) in which case the particle acceleration would not be as strong as assumed in the accretion model. We found no evidence of gamma-ray emission

TABLE 2
SUMMARY OF RESULTS: ASSUMED GAMMA-RAY EMISSION REGION, THRESHOLD ENERGY, AND 2σ UPPER LIMITS.

Cluster	Region	Center		Radius	Threshold	2σ upper limit
		R.A.(J2000)	DEC(J2000)	[deg]	[TeV]	[$\mathrm{cm^{-2}sec^{-1}}$]
Abell 3667	*NW Relic*	$20^h10^m24^s$	$-56°27'00''$	0.30	0.95	3.19×10^{-12}
					1.45	1.64×10^{-12}
					2.05	1.05×10^{-12}
	SE Relic	$20^h14^m36^s$	$-57°03'00''$	0.24	0.85	5.69×10^{-12}
					1.35	1.86×10^{-12}
					2.05	1.55×10^{-12}
	Cluster Core	$20^h12^m27^s.4$	$-56°49'36''$	0.40	0.95	5.52×10^{-12}
					1.35	2.91×10^{-12}
					1.95	2.12×10^{-12}
Abell 4038	*Cluster Core*	$23^h47^m45^s.1$	$-28°08'26''$	0.26	0.75	3.30×10^{-12}
					0.95	2.41×10^{-12}
					1.35	1.57×10^{-12}

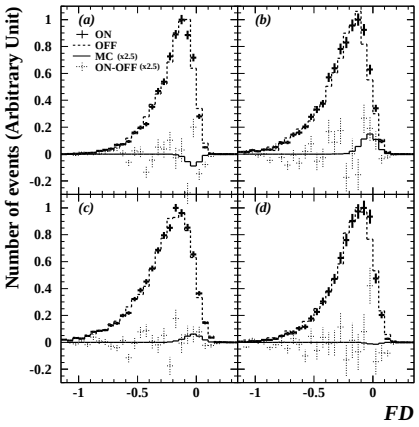

FIG. 3.— *FD* distributions from the four regions. The crosses are *FD* distributions of the ON region, the dashed histograms are those of the OFF region, the dotted crosses are their subtraction (ON−OFF), and the solid histogram is that of gamma rays by Monte-Carlo simulation, which were derived from the fitting procedure : a) the Abell 3667 *NW Relic* region, b) the Abell 3667 *SE Relic* region, c) the Abell 3667 *Cluster Core* region, d) the Abell 4038 *Cluster Core* region. The ON−OFF and gamma ray distributions are magnified by 2.5 for clarity. The resulted gamma-ray flux were at −13%,13%,13% and −0.9% of the Crab-level flux for (a)–(d), where the negative excesses represent statistical fluctuations, and none of the significances exceed 3σ.

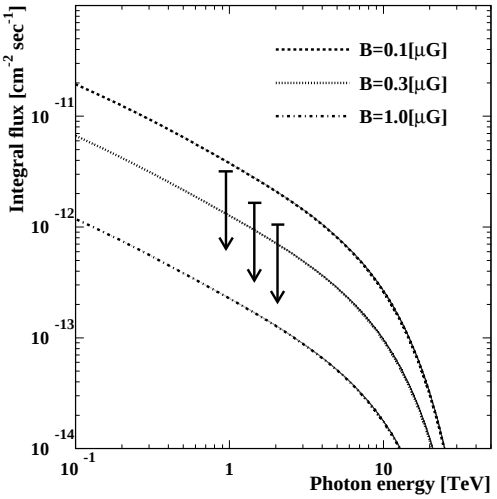

FIG. 4.— Derived gamma-ray flux upper limits from the *NW Relic* region of Abell 3667 (filled squares) with the predicted gamma-ray fluxes by Inoue et al. (2005). The model was scaled with the mass and the distance of Abell 3667 to that of a Coma-like cluster, and is shown in the case of magnetic fields of 0.1μG, 0.3μG, and 1.0μG.

from either region. Since estimations of the magnetic field of Abell 3667 have been made for the area of the cluster center and the north-west relic so far (Johnston-Hollitt 2003), we compared the derived upper limits from *NW Relic* region with the model prediction, as shown in Fig. 4. The model assumes a proton luminosity of one tenth of the kinetic energy flux through strong accretion shocks, which depends on the cluster mass in the form of $\propto M^{5/3}$ (see Eq.(2) in Inoue et al. (2005)), and we scaled the predicted gamma-ray flux according to the mass (M) and distance (d) of Abell 3667 from the (Coma-like cluster) parameters used in their model (M=$2\times10^{15}M_\odot$, d=100 Mpc). The mass of Abell 3667 has been estimated using the Virial relation to be $3.7\times10^{15}M_\odot$ (Sodré et al. 1992) or $1.7\times10^{15}M_\odot$(Girardi et al. 1998), so here we adopt a cluster mass of their mean value, $2.7\times10^{15}M_\odot$. The scaled fluxes are shown in Fig. 4 with lines for magnetic fields of 0.1μG, 0.3μG, and 1.0μG.

Fig. 4 indicates that we can set a lower limit for the magnetic field in the cluster to be $\sim 0.1\mu$G, within the framework of the model by Inoue et al. (2005). This value is not a strong constraint on the magnetic field when it is compared with other estimates, e.g., a few μG from Faraday rotation measurements (see Johnston-Hollitt (2003) for other results); however, the result provides an independent method of a magnetic field estimation, using TeV gamma-ray observations. The flux upper limits from the *SE Relic* region were higher than that of the *NW Relic*, and the lower limit of the magnetic field strength was estimated to be $\sim 0.1\mu$G, depending on the assumed cluster mass. Note that the above flux upper limits also provide a constraint on the gamma-ray emission via primary electron IC emission, which is believed to appear at the shocks (Miniati 2003).

We also searched for gamma-ray emission from the *Cluster Core* regions, deriving flux upper limits. The gamma-ray flux via π^0-decay, produced in hadronic collisions of high-energy protons with the ICM, is thought

to be brightest at the cluster centers, and its flux level is usually discussed from the perspective of an effective confinement of cosmic-rays inside a cluster during the Hubble time. Here, we discuss the total cosmic-ray energy stored inside the cluster centers, using the CANGAROO-III result. We plotted the flux upper limits from the Abell 4038 *Cluster Core* region together with the EGRET upper limit (Reimer et al. 2003) in Fig. 5. We adopted the assumptions of Völk & Atoyan (2000), as introduced in a previous section, and the gamma-ray absorption effect by IR photons (P0.4 model in Aharonian et al. (2006)) was also incorporated. The gamma-ray spectra were represented by lines in Fig. 5, which were scaled to be consistent with the EGRET upper limits.

As shown in Fig. 5, the EGRET & CANGAROO-III results for Abell 4038 gave almost the same constraint on the gamma-ray emission for the case of $\Gamma = -2.1$, and the total cosmic-ray energy to explain our flux upper limits is 1.2×10^{63} erg, using an ICM density of 10^{-3} cm^{-3}, which is a typical value for cluster centers (Blasi et al. 2007). We then derived the upper limit of the cosmic-ray energy density within the *Cluster Core* region of Abell 4038, as $\sim$40eV cm^{-3}, assuming a spherical symmetry with the radius that we defined for this region. The same estimation was applied for the *Cluster Core* region of Abell 3667 as well, and the upper limit was calculated to be $\sim$20eV cm^{-3}. Two factors should be considered for this value: as described in §1, the morphology of Abell 3667 is elongated towards two radio relics, rather than a simple sphere, so the assumption of a spherical symmetry might need to be reexamined where the cluster type of Abell 4038 is cD. Also, if we adopt the XMM results, the search region is effectively a point source, as described beforehand. In this case, a lower flux upper limit is obtained, and the total volume of the search region also decreased, with the cosmic-ray energy density increasing to $\sim$40eV cm^{-3}, which was the same level for Abell 4038. In any case, the derived values are 1 order of magnitude higher than that of our Galaxy, $\sim$1 eV cm^{-3}, opening the door to discussions of the non-thermal component in the clusters. All the calculated upper limits are summarized in Table 3.

Further observations of clusters of galaxies in the TeV-band by next-generation IACTs currently in the planning stage, such as CTA[18] or AGIS[19] , and in the GeV-band by GLAST[20] will open a new window in the research of high-energy phenomena of clusters of galaxies with their improved sensitivities.

6. CONCLUSION

We observed two clusters of galaxies, Abell 3667 and Abell 4038, searching for very-high-energy gamma-ray emission with the CANGAROO-III atmospheric Cherenkov telescope system in 2006. No significant excess was detected from the clusters, and flux upper limits on the gamma-ray emission were obtained. By comparing the upper limit for the north-west radio relic region of Abell 3667 with a model prediction, we can derive a lower limit for the magnetic field of the region of $\sim0.1\mu$G. We also discussed the flux upper limit from the cluster center regions using a gamma-ray emission model via the decay of π^0 produced in hadronic collisions of cosmic-ray protons with the ICM. The upper limit of the cosmic-ray energy density stored within cluster centers was estimated to be $\sim$40eV cm^{-3} by imposing some assumptions, such as the ICM density, and the values are 1 order higher than that of our Galaxy. These estimations show the potential of gamma-ray observations in studies of the cluster environment.

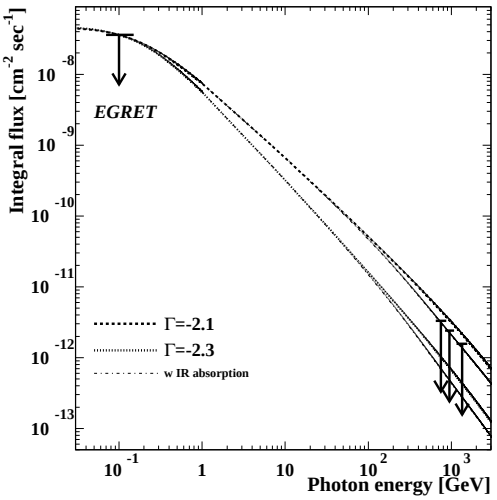

FIG. 5.— Derived gamma-ray flux upper limits from the *Cluster Core* region of Abell 4038 with the gamma-ray emission spectrum via π^0-decay process, normalized to the EGRET upper limits (Reimer et al. 2003). The EGRET upper limits are indicated by arrows at 100 MeV, and the lines are the gamma-ray spectrum from the proton power-law indices of $\Gamma = -2.1$ and -2.3 with an energy cutoff of 200 TeV. The gamma-ray absorption effect by IR photons are represented by dot-dash lines, where the P0.4 model in Aharonian et al. (2006) is adopted.

We thank Dr. S. Inoue for discussions and suggestions on gamma-ray emission from a cluster of galaxies. This work was supported by a Grant-in-Aid for Scientific Research by the Japan Ministry of Education, Culture, Sports, Science and Technology, the Australian Research Council, JSPS Research Fellowships, and the Inter-University Research Program of the Institute for Cosmic Ray Research. We thank the Defense Support Center Woomera and BAE Systems.

[18] http://www.mpi-hd.mpg.de/hfm/CTA/
[19] http://gamma1.astro.ucla.edu/agis/
[20] http://glast.gsfc.nasa.gov/

REFERENCES

Abell, G. O., Corwin., H.G.,Jr., & Olowin, R.P. 1989, ApJS, 70, 1
Aharonian, F. A., et al. 2006, Nature, 440, 1018
Berezinsky, V. S., Blasi, P., & Ptuskin, V. S. 1997, ApJ, 487, 529
Blasi, P., Colafrancesco, S. 1999, Astropart. Phys., 12, 169
Blasi, P., Gabici, S., & Brunetti, G. 2007, Int. J. Mod. Phys. A22, 681
Bowyer, S., Korpela, E., J., Lampton, M., & Jones, T., W. 2004, ApJ, 605, 168

TABLE 3
SUMMARY OF VARIOUS LIMITS ON THE CLUSTERS. THE DEFINED REGIONS, GAMMA-RAY FLUX UPPER LIMITS, LOWER LIMIT OF MAGNETIC FIELD, AND COSMIC-RAY ENERGY DENSITY

Region		2σ upper limit[a] $[cm^{-2}sec^{-1}]$	Magnetic field $[\mu G]$	Energy density $[eV\ cm^{-3}]$
A3667 *NW Relic*		3.19×10^{-12}	>0.1	–
A3667 *SE Relic*		5.69×10^{-12}	>0.1	–
A3667 *Cluster Core*	I.[b]	5.52×10^{-12}	–	<20
	II.[c]	2.03×10^{-12}	–	<40
A4038 *Cluster Core*		3.30×10^{-12}	–	<40

[a]The threshold energy was listed in Table 2.
[b]Based on *ROSAT* data.
[c]Based on XMM-Newton data (point source analysis).

Briel, U. G., Finoguenov, A., & Henry, J. P. 2004, A&A, 426, 1
Condon, J. J., Cotton, W. D., Greisen, E. W., Yin, Q. F., Perley, R. A., Taylor, G. B., Broderick, J. J. 1998, AJ, 115, 1693
Domainko, W., Benbow, W., Hinton, J. A., Martineau-huynh, O., De Naurois, M., Nedbal, D., Pedaletti, G., Rowell, G. 2007, Proc. 30th Int.Cosmic Ray Conf. (Merida), (arXiv:0708.1384)
Edge, A. C., Stewart, G. C., & Fabian, A. C. 1992, MNRAS, 258, 177
Enomoto, R., et al. 2002, Astropart. Phys., 16, 235
Enomoto, R., et al. 2006a, ApJ, 638, 397
Enomoto, R., et al. 2006b, ApJ, 652, 1268
Enßlin, T. A., Biermann, P. L., Klein, U., & Kohle, S. 1998, A&A, 332, 395
Fegan, S. J., et al. 2005, ApJ, 624, 638
Fisher, R. A. 1936, Ann. Eugenics, 7, 179
Fusco-Femiano, R., Fiume, D. D., Orlandini, M., Brunetti, G., Feretti, L., & Giovannini, G. 2001, ApJ, 552, 97
Gabici, S., & Blasi, P., 2004, Astropart. Phys., 20, 579
Giovannini, G., & Feretti, L. 2004, J. Korean Astro. Soc., 37, 323
Girardi, M., Giuricin, G., Mardirossian, F., Mezzetti, M., & Boschin, W. 1998, ApJ, 505, 74
Hattori, T., et al. 2003, Proc. 28th Int. Cosmic Ray Conf. (Tsukuba), 5, 2659
Hillas, A. M. 1985, Proc. 19th Int. Cosmic Ray Conf. (La Jolla), 3, 445
Inoue, S., Aharonian, F. A., & Sugiyama, N. 2005, ApJ, 628, 9
Johnston-Hollitt, M. 2003, in Proc. The Riddle of Cooling Flows in Galaxies and Clusters of Galaxies, edited by T. Reiprich, J. Kempner, and N. Soker, p. 51.
Kabuki, S., et al. 2003, Nucl. Instrum. Meth., A500, 318
Kabuki, S., et al. 2007, ApJ, 668, 968
Kawachi, A., et al. 2001, Astropart. Phys., 14, 261
Kawasaki, W., & Totani, T. 2002, ApJ, 576, 679
Knopp, G. P., Henry, J. P., & Briel, U. G. 1996, ApJ, 472, 125
Kubo, H., et al. 2001, Proc. 27th Int. Cosmic Ray Conf. (Hamburg), 2900
Mauch, T., Murphy, T., Buttery, H. J., Curran, J., Hunstead, R. W., Piestrzynski, B., Robertson, J. G., & Sadler, E. M. 2003, MNRAS, 342, 1117
Miniati, F., Ryu, D., Kang, H., Jones, T. W., Cen, R., & Ostriker, J. P. 2000, ApJ, 542, 608
Miniati, F. 2003, MNRAS, 342, 1009
Mohr, J. J., Mathiesen, B., & Evrard, A. E. 1999, ApJ, 517, 627
Nevalainen, J., Oosterbroek, T., Bonamente, M., & Colafrancesco, S. 2004, ApJ, 608, 166
Nishijima, K., et al. 2005, Proc. 29th Int. Cosmic Ray Conf. (Pune), 5, 327
Ostrowski, M. 2002, Astropart. Phys., 18, 229
Perkins, J. S., et al. 2006, ApJ, 644, 148
Pfrommer, C., & Enßlin, T. A. 2004, A&A, 413, 17 (erratum: 426, 777)
Reimer, O., Pohl, M., Sreekumar, P., & Mattox, J. R. 2003, ApJ, 588, 155
Roettiger, K., Burns, J. O., & Stone, J. M. 1999, ApJ, 518, 603
Rood, H. J., & Sastry, G. 1971, PASP, 83, 313
Röttgering, H. J. A., Wieringa, M. H., Hunstead, R. W., & Ekers, R. D. 1997, MNRAS, 290, 577
Ryu, D., Kang, H., Hallman, E., & Jones, T. W. 2003, ApJ, 593, 599
Scharf, C. A., & Mukherjee, R. 2002, ApJ, 580, 154
Slee, O. B., & Roy, A. L. 1998, MNRAS, 297, 86
Slee, O. B., Roy, A. L., Murgia, M., Andernach, H., & Ehle, M. 2001, AJ, 122, 1172
Sodré, L., Capelato, H. V., Steiner, J. E., Proust, D., & Mazure, A. 1992, MNRAS, 259, 233
Totani, T., & Kitayama, T. 2000, ApJ, 545, 572
Vikhlinin, A., Markevitch, M., & Murray, S. S. 2001, ApJ, 551, 160
Voges, W, et al. 1999, A&A, 349, 389
Völk, H. J., Aharonian, F. A., & Breitschwert, D. 1996, Space Sci. Rev., 75, 279
Völk, H. J., & Atoyan, A. M. 2000, ApJ, 541, 88